Acta Oceanol. Sin., 2014, Vol. 33, No. 8, P. 95–105
DOI: 10.1007/s13131-014-0459-9
http://www.hyxb.org.cn
E-mail: hyxbe@263.net

A numerical model study on multi-species harmful algal blooms coupled with background ecological fields

WANG Qing[1,2,3], ZHU Liangsheng[2], WANG Dongxiao[1]*

[1] State Key Laboratory of Tropical Oceanography, South China Sea Institute of Oceanology, Chinese Academy of Sciences, Guangzhou 510640, China
[2] Naval Architecture and Ocean Engineering R & D Center of Guangdong Province, South China University of Technology, Guangzhou 510640, China
[3] Graduate University of Chinese Academy of Sciences, Beijing 100049, China

Received 25 November 2012; accepted 14 February 2013

Abstract

Based on systematized physical, chemical, and biological modules, a multi-species harmful algal bloom (HAB) model coupled with background ecological fields was established. This model schematically embodied that HAB causative algal species and the background ecological system, quantified as total biomass, were significantly different in terms of the chemical and biological processes during a HAB while the interaction between the two was present. The model also included a competition and interaction mechanism between the HAB algal species or populations. The Droop equation was optimized by considering temperature, salinity, and suspended material impact factors in the parameterization of algal growth rate with the nutrient threshold. Two HAB processes in the springs of 2004 and 2005 were simulated using this model. Both simulation results showed consistent trends with corresponding HAB processes observed in the East China Sea, which indicated the rationality of the model. This study made certain progress in modeling HABs, which has great application potential for HAB diagnosis, prediction, and prevention.

Key words: background ecological fields, multi-species, harmful algal bloom, numerical model

Citation: Wang Qing, Zhu Liangsheng, Wang Dongxiao. 2014. A numerical model study on multi-species harmful algal blooms coupled with background ecological fields. Acta Oceanologica Sinica, 33(8): 95–105, doi: 10.1007/s13131-014-0459-9

1 Introduction

In recent decades, the pollution by human activities in the marine environment has gradually increased. As a result, the areas with marine disasters and environmental issues caused by harmful algal blooms (HABs) have expanded worldwide from a few coastal states in the 1970s (Fig. 1). HABs have long drawn the attention of global research organizations (GEOHAB, 2001; Zhou and Zhu, 2006). Most statistical analyses of in-situ monitoring data assume eutrophication as the main cause of a HAB, for which human activities are also responsible (Sellner et al., 2003; Heisler et al., 2008). However, HABs are an ecologically abnormal phenomenon with complex mechanisms, in which other marine conditions besides eutrophication probably also play some role. At present, a mathematical model based on complete ecosystems is one of the best ways to carry out a reliable prediction of HAB and a comprehensive study of its dynamic mechanisms (Allen et al., 2008).

According to the different ecological variables selected, HAB numerical models can be broadly grouped into three categories of algal blooms, described as total biomass, HAB causative algal species, and causative algal species coupled with background ecological fields.

A typical N-P model is often used for the algal bloom, which is described as the total biomass. In the model, total nutrient level (N) and phytoplankton biomass (P) are the main variables. Based on this type of model, temporal changes of variables, nutrient conditions, temperature effects, and other dynamic mechanisms during the bloom (defined as total biomass) are discussed. In N-P model-related research, most only considered the variation over time without any spatial analysis (Wang, Feng et al., 2002; Huppert et al., 2004, 2005; Freund et al., 2006). In model studies concerning the total biomass, the occurrence of a HAB was estimated as a certain value of chlorophyll concentration, which revealed basic phases of the HAB process from overall development (Wan and Yuan, 1999, 2000; Villanoy et al., 2006). These models, with growth rate, respiratory rate, grazing pressure, and other essential parameters set to empirical values cannot consider the physiological and growth characteristics of HAB species in certain marine environments. It is worth mentioning that in an early model study by Kishi and Ikeda (1986), the seawater movement and its effect on HAB process had been taken into account in the model although still based on an N-P model.

The main method of research for a single or multiple species HAB model is to couple three-dimensional (3-D) hydrodynamic and ecological modules, which is also the main trend of developing marine ecosystem dynamics (Tang et al., 2005). Numerical studies of single species or population HAB models determine the key parameters based on culture experiments and analyze the sensitivity to these parameters and other input conditions (Salacinska et al., 2010). In this manner, the ecosystem in the model is characterized to represent the HAB process

Foundation item: The National Natural Basic Research Program of China (973 Program) under contract No. 2010CB428704.
*Corresponding author, E-mail: dxwang@scsio.ac.cn

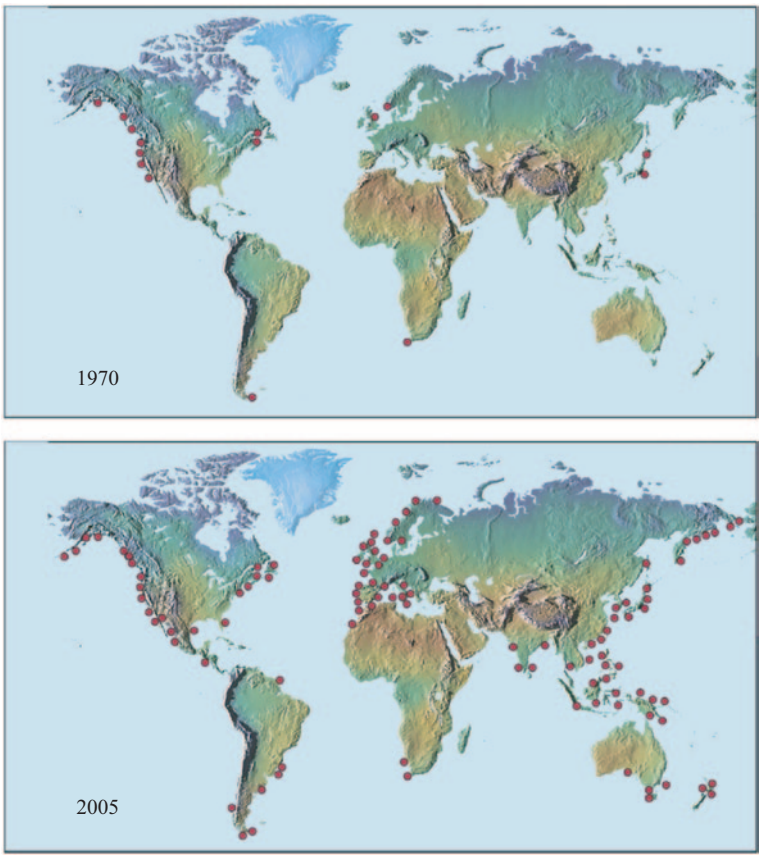

Fig.1. Global expansion in the distribution of paralytic shellfish poisoning (PSP) toxins: 1970 versus 2005. Modified from Anderson (2009).

caused by certain species (Ennet et al., 2000; Chen and Arthur, 2006). By coupling hydrodynamic and ecological modules, not only are the dynamic mechanisms of marine environmental factors (e.g., currents, temperature, salinity, nutrients) included in the model, but the multiplication and distribution characteristics of the HAB species are also analyzed comprehensively (Yanagi et al., 1995; Trancoso et al., 2005). With the increase of marine ecological observations, competition mechanism studies based on the two-population HAB models (Dippner, 1998, Li et al., 2008) have gradually become the hotspot in this field, and the effect of environmental factors on this mechanism has been well noted. With the inclusion of competition and interaction between two algal species or populations, the transformation from a single species to two species completes the ecological mechanism of the HAB model to a certain degree. However, the species or populations in a marine total biomass ecosystem are often much more than two; therefore, the need arises for including multiple species in the HAB model.

The causative species with background ecological fields coupled with the HAB conceptual model considers the microplankton component as a dynamic balance of biological background and includes an independent biological variable of HAB causative species. The numerical simulation of this type of HAB model was also conducted in the area with hydrodynamic characteristics. The Michaelis-Menten equation (Michaelis and Menten, 1913), together with temperature impact factor, was used to parameterize the HAB species growth rate in the study of Wang et al. (2010). This equation is capable of exhibiting the nutrient absorption mechanism, but is not appropriate for application to the algal growth rate, which does not include algal excretion or nutrient threshold. Moreover, the growth of HAB species is controlled not only by nutrients and temperature (Liu et al., 2002; Li, Lv et al., 2005; Lv and Ou, 2006; Ou and Lv, 2006; Wang et al., 2008) but also by salinity and suspended materials as well (Chen et al., 2005; Li, Zhao et al., 2005), which are necessary to be considered. Furthermore, it is not enough for the nutrients, as an important HAB material basis, to be driven only by open boundary conditions. In the case of unclear ecological mechanisms, it is proper to use observations to adjust the source and sink processes of nutrients. From an ideal viewpoint, if the number of algal variations in the model could be changed in the case of unknown causative species during a HAB, different research needs would be met.

Thus, through systematizing physical, chemical, and biological modules, a mathematical HAB model study was conducted based on the mechanism of evident distinction between causative species and background ecological microplankton and on the competitive interaction among multiple possible causative species. A coupled hydrodynamical ecological model for regional shelf seas (COHERENS) (Luyten et al., 1999) was introduced below to build the background ecological fields. The Droop equation (Droop et al., 1982), including the nutri-

ent threshold, was applied as the basic pattern of algal growth combined with temperature, salinity, and suspended material impact factors.

2 Background ecological fields coupled with multi-species HAB theoretical model

In the course of a HAB, the growth rate of causative species far exceeds that of the background microplankton. There exist remarkable differences between chemical and biological processes of HAB species and the background biology that influence each other. Therefore, under the background ecological fields, the growth of HAB species was considered an independent module, which interacts with and influences the background ecology through marine environmental factors. It is based on this mechanism that a multi-species HAB model coupled with background ecological fields was built.

Marine ecological observations suggest there is a competition mechanism between two species or populations with great effects from environmental factors. In order to represent this competition and interaction mechanism among a number of possible causative species, the development of the HAB model from one or two species to multiple species provides a more comprehensive tool to study ecological mechanisms. The physical and chemical-biological parts of this model were built according to the corresponding part of COHERENS. In addition, a corrected term was added to the surface nutrient flux in the model to provide a nutrient environment closer to reality (Gan et al., 1998). The schematic structure of the model is shown in Fig. 2.

Under this structure of the theoretical model, the normal marine environment maintains the HAB species and microplankton of the background ecological system in a relatively balanced state of propagation and consumption. When the temperature, salinity, nutrients, and other environmental variables are suitable for certain HAB species, the HAB propagates rapidly at a much higher growth rate than the balanced state and forms a HAB driven by the seawater aggregation. Similarly, the adaptation of the algae to the environment determines the causative species of the HAB that compete for the resources from environmental factors with a certain spatial and temporal distribution.

2.1 *Physical module*

The governing Eqs (1)–(6) of this module from COHERENS consist of momentum, continuity, temperature, and salinity

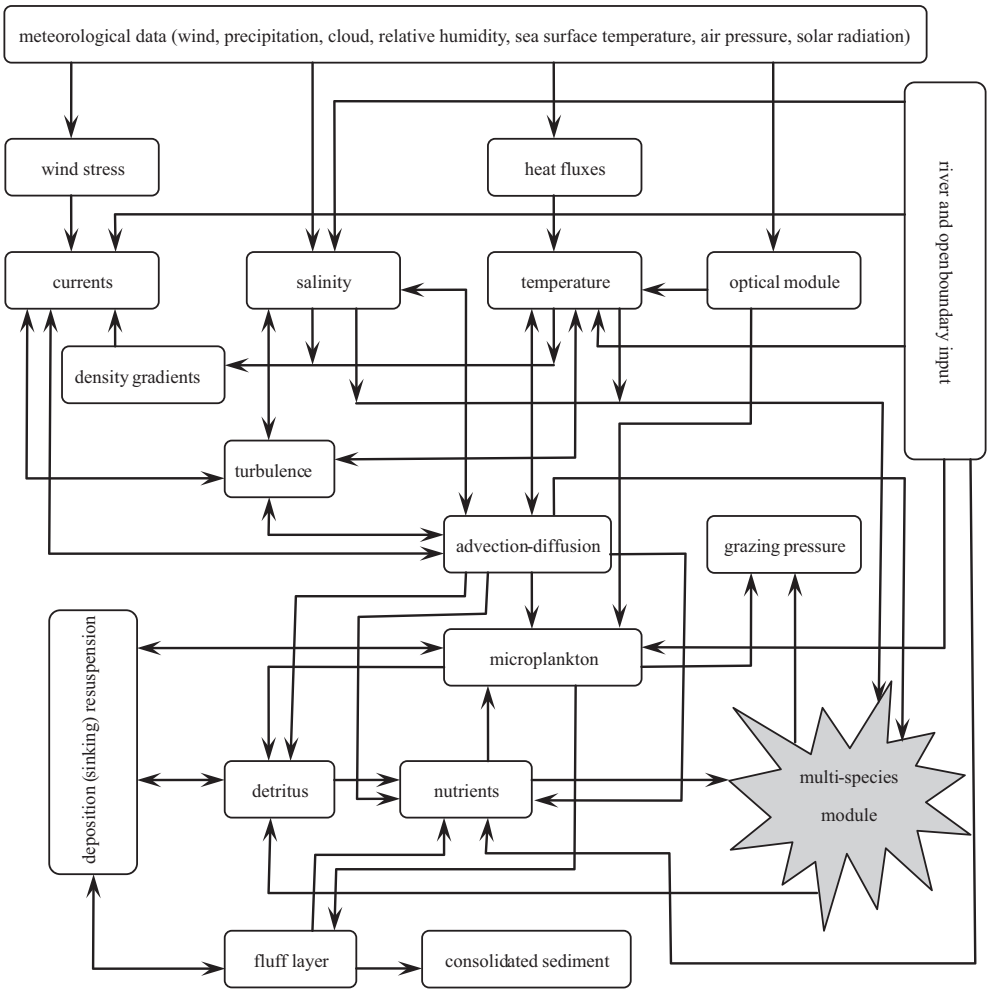

Fig.2. Schematic structure of background ecological fields coupled with the multi-species HAB theoretical model.

equations, as follows:

$$\frac{\partial u}{\partial t}+u\frac{\partial u}{\partial x_1}+v\frac{\partial u}{\partial x_2}+w\frac{\partial u}{\partial x_3}-fv$$
$$=-\frac{1}{\rho_0}\frac{\partial p}{\partial x_1}+\frac{\partial}{\partial x_3}(\nu_T\frac{\partial u}{\partial x_3})+\frac{\partial}{\partial x_1}\tau_{11}+\frac{\partial}{\partial x_2}\tau_{21}, \quad (1)$$

$$\frac{\partial v}{\partial t}+u\frac{\partial v}{\partial x_1}+v\frac{\partial v}{\partial x_2}+w\frac{\partial v}{\partial x_3}+fu$$
$$=-\frac{1}{\rho_0}\frac{\partial p}{\partial x_2}+\frac{\partial}{\partial x_3}(\nu_T\frac{\partial v}{\partial x_3})+\frac{\partial}{\partial x_1}\tau_{12}+\frac{\partial}{\partial x_2}\tau_{22}, \quad (2)$$

$$\frac{\partial P}{\partial x_3}=-\rho g, \quad (3)$$

$$\frac{\partial u}{\partial x_1}+\frac{\partial v}{\partial x_2}+\frac{\partial w}{\partial x_3}=0, \quad (4)$$

$$\frac{\partial T}{\partial t}+u\frac{\partial T}{\partial x_1}+v\frac{\partial T}{\partial x_2}+w\frac{\partial T}{\partial x_3}$$
$$=\frac{1}{\rho_0 c_p}\frac{\partial I}{\partial x_3}+\frac{\partial}{\partial x_3}(\lambda_T\frac{\partial T}{\partial x_3})+\frac{\partial}{\partial x_1}(\lambda_H\frac{\partial T}{\partial x_1})+\frac{\partial}{\partial x_2}(\lambda_H\frac{\partial T}{\partial x_2}), \quad (5)$$

$$\frac{\partial S}{\partial t}+u\frac{\partial S}{\partial x_1}+v\frac{\partial S}{\partial x_2}+w\frac{\partial S}{\partial x_3}$$
$$=\frac{\partial}{\partial x_3}(\lambda_T\frac{\partial S}{\partial x_3})+\frac{\partial}{\partial x_1}(\lambda_H\frac{\partial S}{\partial x_1})+\frac{\partial}{\partial x_2}(\lambda_H\frac{\partial S}{\partial x_2}), \quad (6)$$

where u, v, and w are velocity components of the current, T denotes temperature, S is salinity, f (= $2\Omega\sin\varphi$) is the Coriolis frequency, Ω (= $2\pi/86\,164$ rad/s) is the rotation frequency of the earth, g is the acceleration of gravity, P is the pressure, ν_T and λ_T are the vertical eddy viscosity and diffusion coefficients, respectively, λ_H is the horizontal diffusion coefficient for salinity and temperature, ρ is density, ρ_0 is a reference density, c_p is the specific heat of seawater at constant pressure, and $I(x_1, x_2, x_3, t)$ is the solar irradiance. In the actual integration, a σ-coordinate transformation Eq. (7) is applied in the vertical direction, where ζ is the sea surface elevation and h is the mean water depth so that the total water depth, H, is given by $H = h + \zeta$. The σ-coordinate transformation is as follows:

$$\sigma=\frac{x_3+h}{\zeta+h}=\frac{x_3+h}{H}. \quad (7)$$

The equations are discretized horizontally on a C-grid. We adopted the level 2.5 turbulence closure model of Mellor and Yamada (1982). Horizontal diffusion was determined in an analogy of Smagorinsky (1963). The advective items were evaluated with the total variation diminishing (TVD) scheme using a superbee limiter (Roe, 1985). Note that the temperature equation includes a solar irradiance source term, $\partial I/\partial x_3$, which assigns the sea surface heat flux in accordance with the optical attenuation rule to a certain water depth and influences the temperature in various layers. The absorption of solar heat in the upper water column was performed by the Paulson and Simpson (1977) optical module.

In the physical module, the surface currents were driven by wind stress as a function of the wind components, and the surface fluxes of heat and salinity were parameterized using sea surface air temperature, relative humidity, cloud cover, and other meteorological parameters. The bottom velocity was affected by seabed topography in the horizontal direction and was zero in the vertical direction. The normal fluxes of temperature and salinity and their exchanges at the sea bottom were set to zero, and their exchanges at the sea bottom were also set to zero. A typical radiation condition was applied for the 2-D open boundary condition for currents, and the boundary condition for the 3-D horizontal current was formulated in the form of a prescription for the deviation from the 2-D value. Zero normal gradient condition was applied for all scalars at the open boundary. All fluxes along the coastline were set to zero.

2.2 *Chemical and biological module for background ecological fields*

In the chemical and biological module from COHERENS, concentrations of organic carbon and nitrogen were cycled through microplankton and detrital compartments with associated changes in dissolved concentrations of nitrate, ammonium, and oxygen. The main ecological processes (Fig. 3) involved in this module included microplankton growth and respiration, mesozooplankton grazing and excretion, nutrient uptake, nitrification, detritus generation, and remineralisation. Zooplankton were not simulated but input to the model as a time series of grazing pressure observations, so the ecosystem described by the model was "open" at the second trophic level, where the zooplankton nitrogen variable accumulated potential losses.

This module contained eight state variables: microplankton carbon (B) and nitrogen (N), detrital carbon (C) and nitrogen (M), concentrations of dissolved nitrate (^{NO}S), ammonium (^{NH}S), and oxygen (O), and accumulated zooplankton nitrogen

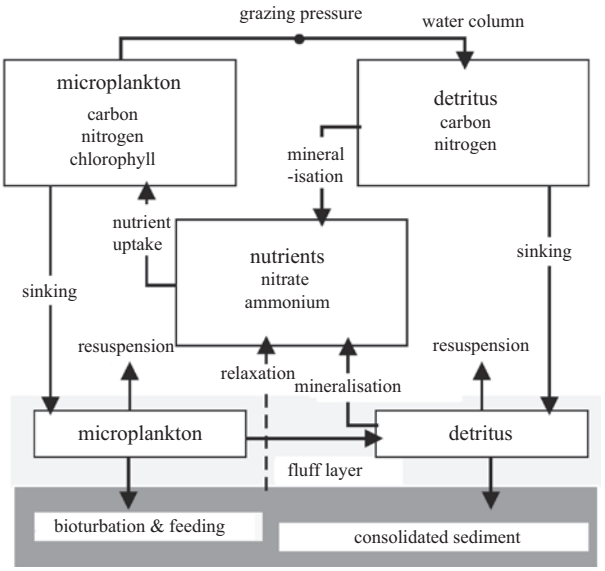

Fig.3. Chemical and biological module structures. Modified from Luyten et al. (1999).

(Z_N). The concentrations were updated at each time step by solving a transport Eq. (8) for each state variable, whereby the biological interactions were included as source and sink terms according to Eqs (9)–(16), which take into account vertical sinking and physical transport by advection and diffusion, as follows:

$$\frac{\partial \psi}{\partial t}+\frac{\partial(u\psi)}{\partial x_1}+\frac{\partial(v\psi)}{\partial x_2}+\frac{\partial(w\psi)}{\partial x_3}+\omega_s\frac{\partial \psi}{\partial t}-\frac{\partial}{\partial x_3}(\lambda_T\frac{\partial \psi}{\partial x_3})-\frac{\partial}{\partial x_1}(\lambda_H\frac{\partial \psi}{\partial x_1})-\frac{\partial}{\partial x_2}(\lambda_H\frac{\partial \psi}{\partial x_2})=\beta(\psi), \quad (8)$$

where ω_s is a "non-physical" sinking (or swimming) rate specific for variable ψ, λ_T is the vertical diffusion coefficient, λ_H is the horizontal diffusion coefficient, and $\beta(\psi)$ is the source/sink term. The source/sink term of each state variable is defined as:

$$\beta(B)=(\mu-G)B, \quad (9)$$

$$\beta(N)=({}^{NO}u+{}^{NH}u)B-GN, \quad (10)$$

$$\beta(C)=(1-\gamma)GB-{}^{C}rC, \quad (11)$$

$$\beta(M)=(1-\gamma)GN-{}^{M}rM, \quad (12)$$

$$\beta(Z_N)=\gamma(1-e)GN, \quad (13)$$

$$\beta({}^{NO}S)=C^{NO}uB+{}^{NH}r\cdot{}^{NH}S, \quad (14)$$

$$\beta({}^{NH}S)=-{}^{NH}uB-{}^{NH}r\cdot{}^{NH}S, \quad (15)$$

$$\beta(O)=({}^{O}q^{B}\mu+{}^{O}q^{NO}\cdot{}^{NO}u-{}^{O}q^{C}e\gamma G)B-{}^{O}q^{NH}\cdot{}^{NH}r\cdot{}^{NH}S-{}^{O}q^{C}\cdot{}^{C}rC. \quad (16)$$

The descriptions of parameters and variables of Eqs (9)–(16) are listed in Table 1. Microplankton growth rate was calculated on the basis of threshold limitation and took the minimum value between light-controlled growth rate and nutrient-controlled growth rate. The flux of dissolved nutrients into or out of the sediment was regulated as a relaxation function and no bottom flux of oxygen was assumed. Microplankton state variables were lost to the consolidated sediment at a rate of 10% per day. The surface oxygen flux was related to both wind speed and sea surface temperature. All other surface fluxes were set to zero. The lateral boundary conditions in this module were in accordance with those in the physical module.

2.3 *Multiple HAB species model*

When an algal bloom occurs, the growth rates of causative algal species are much higher than the average growth rate of the background ecology. There exists a competition and interaction mechanism between these causative species. Under the background ecological fields from Section 2.2, the biological process of these possible causative algal species was considered as an independent module, in which the type and number of these species were determined according to the analysis of marine observations. The marine environmental factors, such as currents, nutrients, temperature, salinity, suspended materials and so on, played roles in connecting this module with the background biological fields. The general form of the scalar advection-diffusion equation was adopted for the concentration of causative species, which can be written as follows:

$$\frac{\mathrm{d}AX_i}{\mathrm{d}t}-diff(AX_i)=(\mu_{AX_i}f_i(T)f_i(S)f_i(\mathrm{sed})-G_i)\cdot AX_i, \quad (17)$$

where subscript i denotes the type of algal species; AX_i is the algal concentration (mmol/m^3); μ_{AX_i} is the algal growth rate (d^{-1}); $f_i(T)$, $f_i(S)$, and f_i(sed) are temperature, salinity, and suspended material impact factors, respectively; and G_i is the grazing pressure (d^{-1}). The source/sink part of algal species can be described as the biomass change caused by net growth and mesozooplankton grazing. With the growth mechanism well known, all of the possible causative HAB species in the waters concerned could be theoretically included in this model, of which the multiple possible causative species coexisting mechanism provided an effective numerical study on the HAB when the causative species were unclear.

From the results of algal culture (Wang et al., 2006; Zhao et al., 2009) and mesocosm experiments (Li et al., 2003), it can be concluded that nutrients, temperature, and salinity are the vital environmental resources in the competition mechanism between any two species. Different ranges of adaptation to the nutrients, temperature, and salinity determine the distinction between algal reproductive processes. Therefore, the temperature and salinity curves, together with the nutrient thresholds, were included in this model and parameterized as below.

Table 1. Parameters for source/sink terms in the chemical and biological modules

Symbol	Unit	Description
μ	d^{-1}	microplankton growth rate
G	d^{-1}	grazing pressure
${}^{NO}u$	(mmol N)/[(mmol C)·d]	nitrate uptake rate by microplankton
${}^{NH}u$	(mmol N)/[(mmol C)·d]	ammonium uptake rate by microplankton
γ	—	fraction of the grazed microplankton carbon and nitrogen assimilated by zooplankton
${}^{C}r$	d^{-1}	detrital carbon remineralisation rate
${}^{M}r$	d^{-1}	detrital nitrogen remineralisation rate
${}^{NH}r$	d^{-1}	nitrification rate
${}^{O}q^{B}$, ${}^{O}q^{C}$	(mmol O)/(mmol C)	photosynthetic and respiratory quotient for microplankton carbon growth and detrital respiration
${}^{O}q^{NO}$, ${}^{O}q^{NH}$	(mmol O)/(mmol N)	photosynthetic and respiratory quotient for nitrate uptake and nitrification
e	—	portion of the assimilated nitrogen excreted as ammonium

The temperature and salinity factors were parameterized by an improved form of the Eppley (1972) empirical formula as follows:

$$f_i(T) = e^{-q_T|T-T_r|}, \tag{18}$$

$$f_i(S) = e^{-q_S|S-S_r|}, \tag{19}$$

where q_T and q_S are empirical coefficients, and T_r and S_r are the reference temperature and salinity, respectively. In addition to the temperature and salinity impact factors, the suspended solids impact factors were included in the algal growth mechanism, which to some extent improved the environmental effect mechanism of algal growth. The factor f_i(sed) was assumed as an adjustable parameter related to the location in the water due to the uncertain mechanism of the suspended material effect on algal growth.

The Droop equation combined with the minimum rule was selected to parameterize algal growth in the form given below:

$$\mu_{AX_i} = \mu_{AX_i,\max} \min\left(\frac{C_{N_j} - C_{N_j,\min}}{C_{N_j}}\right), \tag{20}$$

where $\mu_{AX_i,\max}$ is the maximum algal growth rate, C_{N_j} is the concentration (mmol/m^3) of nutrients, subscript j is used as a marker of nutrient type, and $C_{N_j,\min}$ is the nutrient threshold for algal growth.

Due to the uncertainty of limiting nutrients in this area, two variables of phosphate and silicate, together with their equations, which were still in the form of Eq. (8), were added into the multiple species module. However, these two variables were not cycled in the background ecological system but consumed by the background microplankton. Since the nutrient cycle mechanism was not complete, a simple relaxation function (Gan et al., 1998) was applied to correct the surface nutrient fluxes. As the multiple possible causative species model was built, the corresponding consumption was added into the nutrient source/sink term in the background ecological module. As a result, the nutrient source/sink terms were updated to become:

$$\beta(\text{üüüüüüü}) = - \quad uB - \quad r \cdot \quad S - \sum_{i=1}^{N} \quad u_{AX_i} \cdot AX_i + \gamma_{\text{A}} H(\quad S - \quad S), \tag{21}$$

$$\beta(\text{üüüüüüü}) = - \quad uB - \quad r \cdot \quad S - \sum_{i=1}^{N} \quad u_{AX_i} \cdot AX_i + \gamma_{\text{A}} H(\quad S - \quad S), \tag{22}$$

$$\beta({}^{\text{NO}}S) = -{}^{\text{PO}}uB - \sum_{i=1}^{N} {}^{\text{PO}}u_{AX_i} \cdot AX_i + \gamma_{\text{A}} H({}^{\text{PO}}S^* - {}^{\text{PO}}S), \tag{23}$$

$$\beta({}^{\text{SIO}}S) = -{}^{\text{SIO}}uB - \sum_{i=1}^{N} {}^{\text{SIO}}u_{AX_i} \cdot AX_i + \gamma_{\text{A}} H({}^{\text{SIO}}S^* - {}^{\text{SIO}}S), \tag{24}$$

where ${}^{\text{NH}}u_{AX_i}$, ${}^{\text{NO}}u_{AX_i}$, ${}^{\text{PO}}u_{AX_i}$, and ${}^{\text{SIO}}u_{AX_i}$ are ammonium, nitrate, phosphate, and silicate absorption rates of algal species, respectively; ${}^{\text{PO}}S$ and ${}^{\text{SIO}}S$ are phosphate and silicate concentrations, respectively; ${}^{\text{NH}}S^*$, ${}^{\text{NO}}S^*$, ${}^{\text{PO}}S^*$, and ${}^{\text{SIO}}S^*$ are observed values of corresponding nutrients; and γ_{A} is an adjustable relaxation coefficient (d^{-1}).

The boundary conditions at the surface, bottom, and lateral directions in this model were defined in the same way as the COHERENS biological module (Luyten et al., 1999).

3 Simulation of background ecological field in the East China Sea

3.1 *Model configuration and parameter selection*

The model domain (24.5°–41°N, 117°–131°E) of the background ecological fields was located in the East China Sea (ECS). The horizontal resolution was 5′ × 5′, and 11 sigma levels were used vertically. The 2-D time step was 25 s and the 3-D time step was 250 s. Five open boundaries were specified in the Changjiang River (Yangtze River) Estuary (31°00′–31°27′N, 121°33′E), Osumi–Tokara Strait (28°30′–31°00′N, 129°00′–131°00′E), Tsushima Strait (33°30′–35°00′N, 129°00′–130°00′E), and Taiwan Strait and east of Taiwan (117°00′–123°00′E) along 24°30′N. The Ryukyu Island Chain was simplified as a solid boundary. Bathymetry of the model domain and open boundary locations are shown in Fig. 4.

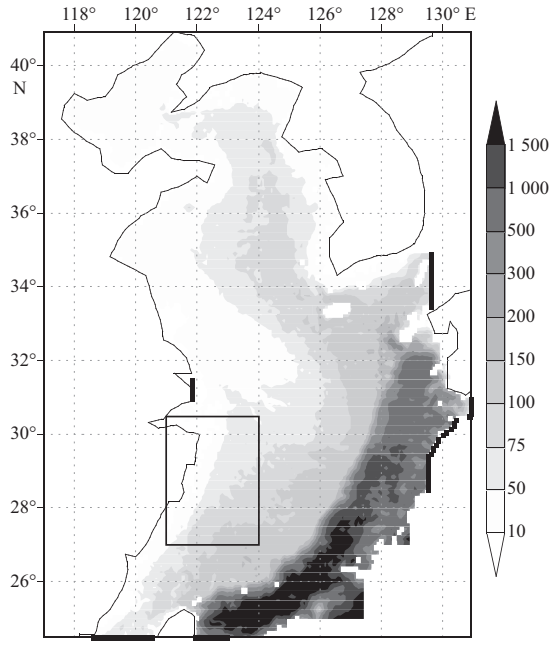

Fig.4. Bathymetry (m) of the model domain and open boundary locations marked with thick solid lines. The small box is used to indicate the area used for HAB simulation.

The temperature and salinity data for the initial and boundary conditions were interpolated from the climatological monthly-mean *World Ocean Atlas 2001* (Conkright et al., 2002; Boyer et al., 2005). The initial fields of microplankton carbon (B) and nitrogen (N) and detrital carbon (C) and nitrogen (M) were distributed according to a certain proportion of WOA2001 chlorophyll data (Conkright et al., 2002). The initial ammonium, nitrate, and dissolved oxygen concentrations were obtained by interpolating the WOA2005 data (Garcia et al., 2006a, b) to the model grid. The runoff from the Changjiang River Estuary came

from the multi-year monthly-mean data of 1990–2004 records in Datong hydrological station, and the nutrient concentrations were set to a high level of 25 mmol/m^3 nitrate, 0.8 mmol/m^3 phosphate and 30 mmol/m^3 silicate.

Due to the lack of related information in the model domain, all parameters in the background ecological module were set to the default values of COHERENS and the ecological simulation results below were analyzed only in the Changjiang River Estuary and its adjacent waters (see the small box in Fig. 4). The simulation was started from a state of rest, together with the climatological monthly-mean temperature and salinity fields from April. Driven by open boundary conditions and surface forcing fields, the simulation was integrated for 360 model days to obtain stable background ecological fields of the ECS in spring.

3.2 *Results and analyses*

3.2.1 *Currents*

Judging from the currents in Fig. 5, the path and scale of the Kuroshio were relatively stable and the Kuroshio intrusion was found at both surface and subsurface layers. The Taiwan Warm Current extended to near the Changjiang River Estuary with the support of the Kuroshio intrusion. There existed obvious directional change of the Changjiang River diluted water, while the Fujian–Zhejiang Coastal Current was weak. The circulation characteristic in this area was basically seen in the model result, which was in a better accordance with the simulated circulation trend, especially in the Changjiang River and its adjacent waters.

3.2.2 *Nutrients*

The distribution of simulated nutrient concentrations in Fig. 6 was basically the same as the spatial distribution: it gradually decreased from the center of the Changjiang River Estuary toward the offshore area. The maximum concentrations of nitrate, phosphate, and silicate were 20, 0.6, and 21 mmol/m^3, respectively, which were all found in the Changjiang River Estuary.

3.2.3 *Microplankton*

The microplankton concentration (Fig. 7) simulated in the model remained at a relatively low level with no obvious spatial feature. The maximum concentration of 0.4 mmol/m^3 appeared outside the Changjiang River Estuary and Zhejiang coastal area. The chlorophyll distribution in this area was mostly consistent with the microplankton, which was also at a low level.

4 Simulation of single species HAB process

4.1 *Species type selection and model configuration*

Prorocentrum donghaiense has been one of the most frequent HAB causative species in the Changjiang River Estuary and its adjacent waters in recent years. It is considered a single species for simulation. *P. donghaiense* parameters were valued according to related research (Table 2). In the absence

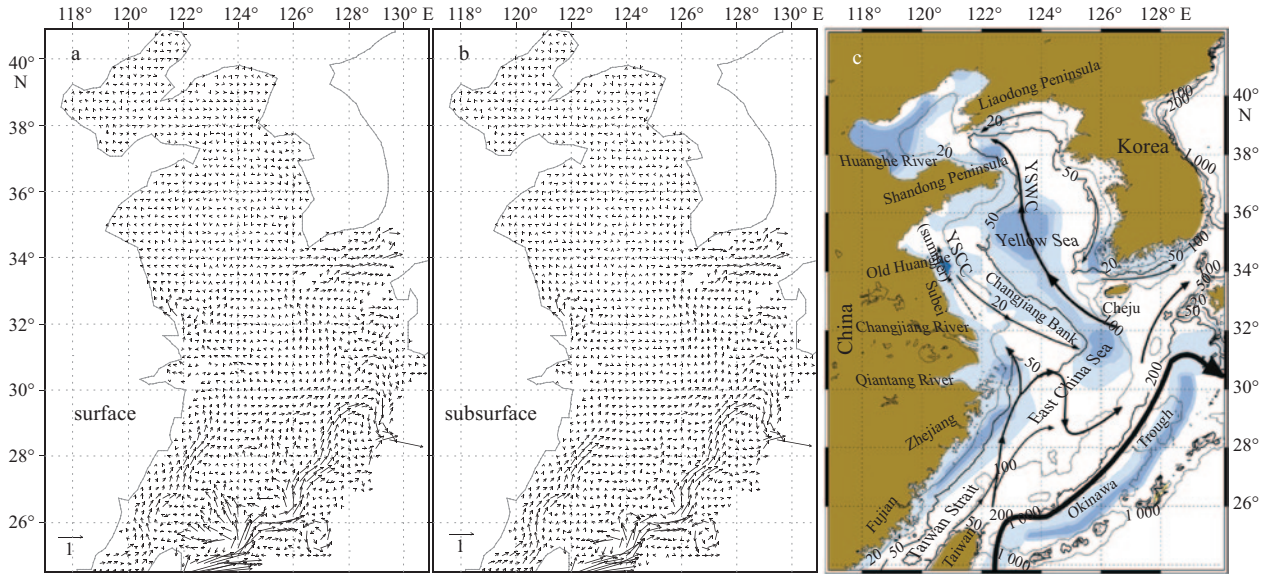

Fig.5. Currents (m/s) of the ECS in spring (a and b) and circulation characteristics (c, modified from Yuan et al. (2008)).

Table 2. *P. donghaiense* parameters

Symbol	Name	Value	Reference
μ_{apdmax}	maximum growth rate	1.88 d^{-1}	Li et al. (2003)
q_T	temperature empirical coefficients	0.7	Chen (2006)
T_r	reference temperature	20°C	Lu et al. (2003); Chen et al. (2005)
q_S	salinity empirical coefficients	0.3	Chen (2006)
S_r	reference salinity	30	Chen (2006)

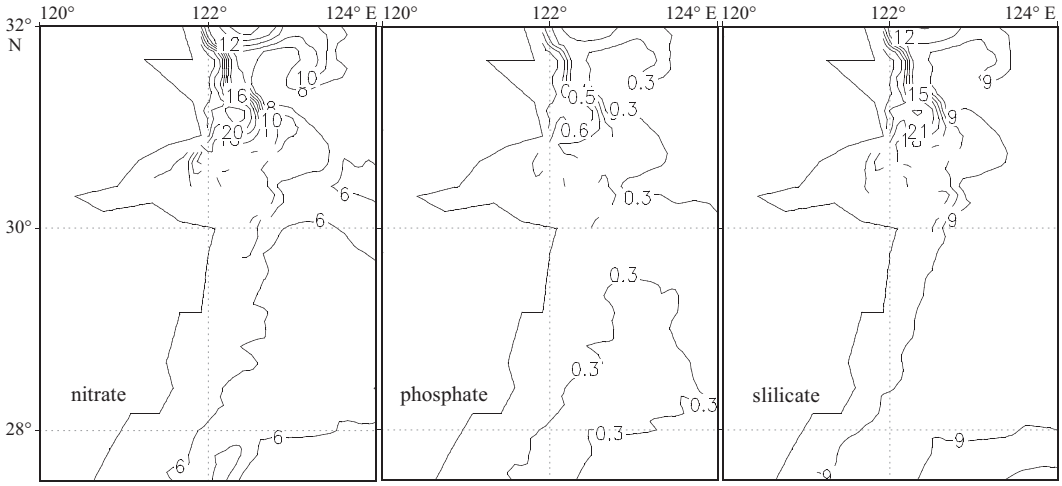

Fig.6. Surface nutrient concentrations (mmol/m^3) in spring.

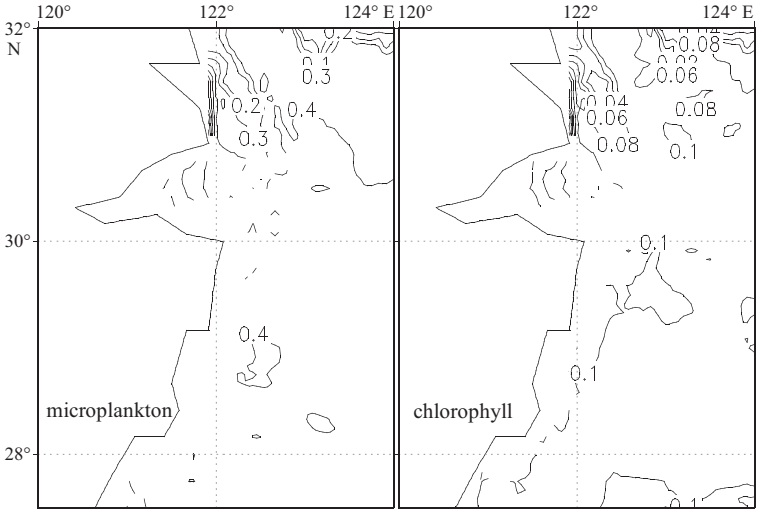

Fig.7. Surface microplankton carbon concentration (mmol/m^3) and chlorophyll concentration (mg/m^3).

of relevant research, the *P. donghaiense* nutrient threshold and uptake rate were free to be adjusted. In line with the concentration characteristics of the occurrence position during the *P. donghaiense* HAB, the single species simulation area was limited in the Changjiang River Estuary and Zhejiang coastal area (27°00′–30°30′N, 121°00′–124°00′E; Fig. 3). The initial concentration of *P. donghaiense* was obtained from the observations of the National 973 Project and the concentrations of nutrients and suspended materials were taken from the field investigation (Wang, Zhan et al., 2002). The open boundary conditions were provided by the background ecological field simulation in Section 3. The *P. donghaiense* HAB process in spring was simulated for 55 model days (April 1–May 25, 2004).

4.2 *Simulation results of P. donghaiense HAB process*

A small area of *P. donghaiense* HAB appeared in the southern coastal area on April 5, which was the fifth day of the model integration. With *P. donghaiense* concentration accumulated for 10 d, a large-scale HAB broke out on April 15. The high value center tended to move northward. On May 15, the HAB center already moved to the open sea outside Hangzhou Bay. In addition to the Taiwan Warm Current, the high level of nutrients around the Changjiang River Estuary made a certain contribution as well to the northward migration of the HAB center. After a maintenance period of 30 model days, the *P. donghaiense* HAB gradually began to disperse. The simulation (Fig. 8) represented the developing trend of the *P. donghaiense* HAB process that occurred from April to May and the northward migration of the HAB center from the southern Zhejiang coastal area to the northern open sea, which was qualitatively in accordance with the survey results (Chen et al., 2006).

5 Simulation of two species HAB process

5.1 *Species type selection and model configuration*

The two causative species in this simulation were assumed

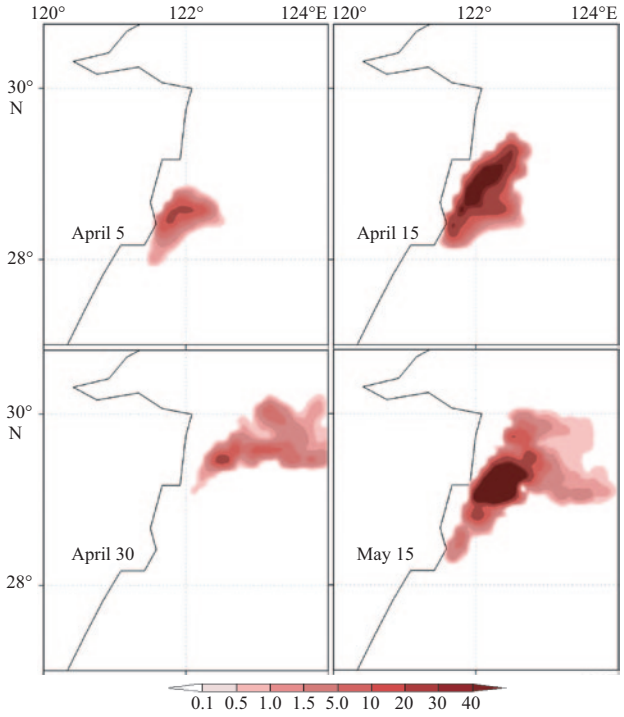

Fig.8. Surface *P. donghaiense* concentration (mmol/m^3).

as *Skeletonema costatum* and *P. donghaiense*, which most frequently trigger a HAB in the ECS. The configuration of *P. donghaiense* was the same as that in Section 4.1. The *S. costatum* parameters were determined according to relevant research (Table 3). The nutrient threshold and uptake rate of *S. costatum* were dealt with in analogy to that in Section 4.1. The initial concentrations of these two species came from in-situ data (Chen et al., 2006; Xie, 2006). The surface nutrient concentration observations were from the field investigation results (Zhang et al., 2008). The two species HAB simulation was performed for 90 model days from March 26 to June 23, 2005.

5.2 *Simulation results of S. costatum and P. donghaiense HAB processes*

Early in the simulation (Fig. 9), *S. costatum* had a visible advantage in terms of concentration. In the eutrophic waters, *S. costatum* HAB broke out in a large area on April 2. It lasted for 23 model days and faded away on April 25. The main reason for the dissipation of the *S. costatum* HAB was probably that the concentrations of nutrients largely consumed in this region decreased to a relatively low level. Possibly because the sea surface temperature (SST) was outside the adaptive temperature range of this organism, the concentration of *P. donghaiense* remained at a very low level during the *S. costatum* HAB and did not start to increase until the *S. costatum* HAB disappeared. In a long gestation period, the *P. donghaiense* HAB occurred on May 9 and dissipated on June 19, lasting nearly 41 model days. By and large, the simulation represented the main features of dominant HAB species succession as diatom–dinoflagellate–diatom, as found by Zhang et al. (2008) in the survey.

The influence of nutrients, temperature, and salinity on HABs in these two simulations can be summarized in the following points. The lack of nutrient supplements in the open sea limited HAB occurrences in the coastal waters. *S. costatum* has a strong dependence on nutrient availability, while *P. donghaiense* can survive under nutrient-limited conditions. The concentration of *S. costatum* continued to decline at the end of the *P. donghaiense* HAB, indicating the model developed here was relatively sensitive to temperature. The salinity in this model had little effect on the HAB process.

6 Conclusions

As primary producers, marine algae bring energy from the non-biological environment into the chain of an entire marine ecosystem. The microplankton ecosystem, interacting directly or indirectly with the algae under certain regulation mecha-

Table 3. *S. costatum* parameters

Symbol	Name	Value	Reference
μ_{max}	maximum growth rate	4.21 d^{-1}	Li et al. (2003)
q_T	temperature empirical coefficients	0.7	Chen (2006)
T_r	reference temperature	17°C	Wang et al. (2006)
q_S	salinity empirical coefficients	0.3	—
S_r	reference salinity	19	Li, Zhao et al. (2005)

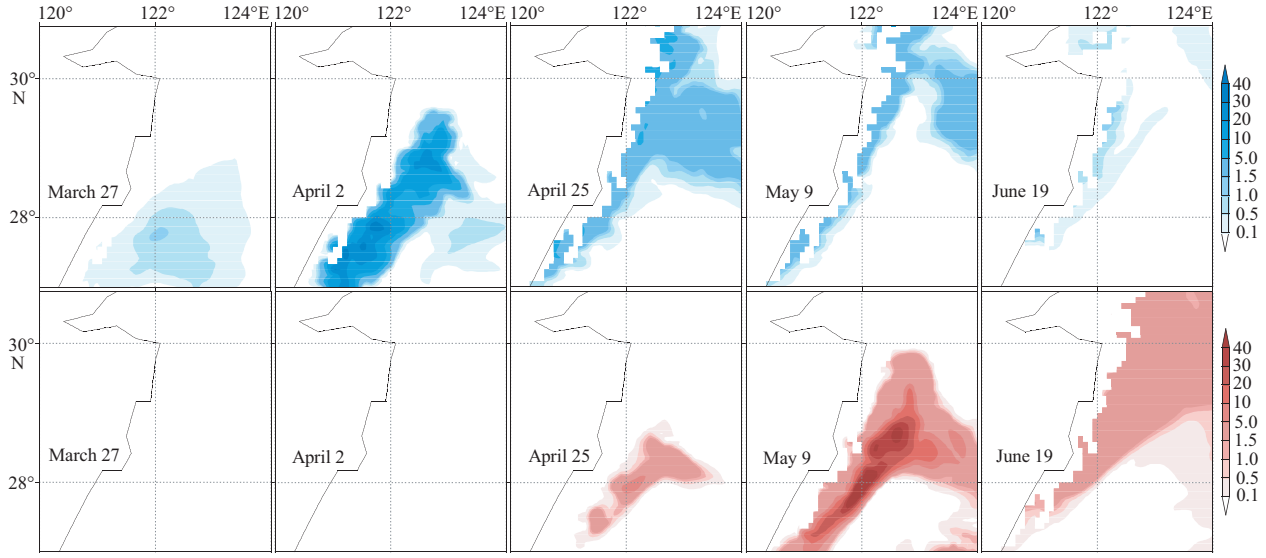

Fig.9. Surface concentrations (mmol/m^3) of *S. costatum* (upper panels) and *P. donghaiense* (lower panels).

nisms, cannot be ignored in the course of a HAB. Therefore, through systematizing physical, chemical, and biological modules, we first built a multiple species module in the form of a number of coexisting HAB causative species. Then, by combining the temperature, salinity, and suspended material impact factors, we conducted a numerical study on multi-species HABs coupled with background ecological fields.

The model revealed the significant difference between HAB causative algal species and background ecological system quantified as a total biomass in the chemical and biological processes during a HAB and the interaction mechanism between them. The algal growth rate was parameterized by applying the Droop equation to include the nutrient threshold in the model, which also considered the effects of temperature, salinity, and suspended materials. The HAB causative species coexisting mechanism can be used to determine the actual causative species during a HAB. The simulation of background ecology in the ECS provided a background field with physical, chemical, and biological characteristics. The single species and two species HAB simulations showed the same evolutions of HAB processes and population succession as the analysis of the field data, showing the capability of this HAB model. The model had an important significance in HAB numerical simulation, for diagnostic study on HABs and for HAB prediction and prevention.

The suspended materials impact factor could be developed to a sediment module according to the light control mechanism on the growth of algal species, which would transform the effect of suspended materials into a light attenuation mechanism included in the background ecosystem. On the basis of more comprehensive research on physiological and ecological mechanisms, the cycles of nitrogen, phosphorus, and silicon in the background ecological microplankton and multiple species module could be complete.

References

Allen J I, Smyth T J, Siddorn J R, et al. 2008. How well can we forecast high biomass algal bloom events in a eutrophic coastal sea. Harmful Algae, 8(1): 70–76

Anderson M D. 2009. Approaches to monitoring, control and management of harmful algal blooms. Ocean & Coastal Management, 52(7): 342–347

Boyer T, Levitus S, Garcia H, et al. 2005. Objective analyses of annual, seasonal, and monthly temperature and salinity for the World Ocean on a 0.25° grid. International Journal of Climatology Early View, 25(7): 931–945

Chen Xiuhua. 2006. Numerical experiments of the development of red tides in the region where red tides frequently occurred in the East China Sea [dissertation]. Guangzhou: South China Sea Institute of Oceanology

Chen Qiuwen, Arthur E M. 2006. Modelling algal blooms in the Dutch coastal waters by integrated numerical and fuzzy cellular automata approaches. Ecological Modelling, 199: 73–81

Chen Hanlin, Lv Songhui, Zhang Chuansong, et al. 2006. A Survey on the red tide of *Prorocentrum donghaiense* in East China Sea 2004. Ecologic Science (in Chinese), 25(3): 226–230

Chen Bingzhang, Wang Zongling, Zhu Mingyuan, et al. 2005. Effects of temperature and salinity on growth of *Prorocentrum dentatum* and comparisons between growths of *Prorocentrum dentatum* and *Skeletonema costatum*. Advances in Marine Science (in Chinese), 23(1): 60–64

Conkright M E, Locarnini R A, Garcia H E, et al. 2002. World Ocean Atlas 2001: Objective Analyses, Data Statistics, and Figures, CD-ROM Documentation. Silver Spring, MD: National Oceanographic Data Center, 1–17

Dippner J W. 1998. Competition between different groups of phytoplankton for nutrients in the southern North Sea. Journal of Marine Systems, 14(1): 181–198

Droop M R, Mickelson M J, Scott J M, et al. 1982. Light and nutrient status of algal cells. Journal of the Marine Biological Association of the United Kingdom, 62(2): 403–434

Ennet P, Kuosa H, Tamsalu R. 2000. The influence of upwelling and entrainment on the algal bloom in the Baltic Sea. Journal of Marine Systems, 25: 359–367

Eppley R W. 1972. Temperature and phytoplankton growth in the sea. United States Fisheries and Wildlife Service Bulletin, 70(4): 1063–1085

Freund A J, Mieruch S, Scholze B, et al. 2006. Bloom dynamics in a seasonally forced phytoplankton-zooplankton model: Trigger mechanisms and timing effects. Ecological Complexity, 3(2): 129–139

Gan Jianping, Mysak L A, Straub D N. 1998. Simulation of the South Atlantic Ocean circulation and its seasonal variability. Journal of Geophysical Research, 103(C5): 10241–10251

Garcia H E, Locarnini R A, Boyer T P, et al. 2006a. World Ocean Atlas 2005, Vol. 4: Nutrients (phosphate, nitrate, silicate). In: Levitus S, ed. NOAA Atlas NESDIS 64, U.S. Washington, DC: Government Printing Office, 1–396

Garcia H E, Locarnini R A, Boyer T P, et al. 2006b. World Ocean Atlas 2005, Vol. 3: Dissolved oxygen, apparent oxygen utilization, and oxygen saturation. In: Levitus S, ed. NOAA Atlas NESDIS 63, U.S. Washington, DC: Government Printing Office, 342

GEOHAB. 2001. Global Ecology and Oceanography of Harmful Algal Blooms Science Plan. Baltimore and Paris: SOR and IOC, 86

Heisler J, Glibert P M, Burkholder J M, et al. 2008. Eutrophication and harmful algal blooms: A scientific consensus. Harmful Algae, 8(1): 3–13

Huppert A, Blasius B, Olinky R, et al. 2005. A model for seasonal phytoplankton blooms. Journal of Theoretical Biology, 236(3): 276–290

Huppert A, Olinky R, Stone L. 2004. Bottom-up excitable models of phytoplankton blooms. Bulletin of Mathematical Biology, 66(4): 865–878

Kishi M, Ikeda S. 1986. Population dynamics of 'red tide' organisms in eutrophicated coastal waters—Numerical experiment of phytoplankton bloom in the East Seto Inland Sea, Japan. Ecological Modelling, 31(1): 145–174

Li Ying, Lv Songhui, Xu Ning, et al. 2005. The utilization of *Prorocentrum donghaiense* to four different types of phosphorus. Ecologic Science (in Chinese), 24(4): 314–317

Li Yanbin, Wang Xiulin, Han Xiurong, et al. 2008. An ecosystem model of the phytoplankton competition in the East China Sea, as based on field experiments. Hydrobiologia, 600(1): 283–296

Li Jingtao, Zhao Weihong, Yang Dengfeng, et al. 2005. Effect of turbid water in Changjiang (Yangtze) estuary on the growth of *Skeletonema costatum*. Marine Sciences (in Chinese), 29(1): 34–37

Li Ruixiang, Zhu Mingyuan, Wang Zongling, et al. 2003. Mesocosm experiment on competition between two HAB species in East China Sea. Chinese Journal of Applied Ecology (in Chinese), 14(7): 1049–1054

Liu Dongyan, Sun Jun, Chen Zongtao, et al. 2002. Effect of N/P ratio on the growth of a red tide diatom *Skeletonema costatum*. Transaction of Oceanology and Limnology (in Chinese), 2: 39–44

Lu Douding, Qi Yuzao, Goebel J, et al. 2003. Redescription of *Prorocentrum donghaiense* Lu and comparison with relevant *Prorocentrum* species. Chinese Journal of Applied Ecology, 14(7): 1060–1064

Luyten P J, Jones J E, Proctor R, et al. 1999. COHERENS-A Coupled Hydrodynamical-Ecological Model for Regional and Shelf Seas: User Documentation. MUMM Report, Management Unit of the Mathematical Models of the North Sea, 1–914

Lv Songhui, Ou Meishan. 2006. Effects of different nitrogen sources and N/P ratios on the growth of a marine dinoflagellate *Prorocentrum donghaiense*. Marine Environmental Science (in Chinese), 25(2): 33–36

Mellor G L, Yamada T. 1982. Development of a turbulence closure model for geophysical fluid problems. Reviews of Geophysics and Space Physics, 20(4): 851–875

Michaelis L, Menten M L. 1913. Die kinetik der invertinwirkung. Biochem Z, 49: 333–369

Ou Meishan, Lv Songhui. 2006. Effects of different inorganic nitrogen sources on the growth of *Prorocentrum donghaiense*. Ecologic Science (in Chinese), 25(1): 28–31

Paulson C A, Simpson J J. 1977. Irradiance measurements in the upper ocean. Journal of Physical Oceanography, 7(6): 952–956

Roe P L. 1985. Some contributions to the modelling of discontinuous flows. Lectures in Applied Mathematics, 22: 163–193

Salacinska K, Serafy G Y, Los F J, et al. 2010. Sensitivity analysis of the two dimensional application of the Generic Ecological Model (GEM) to algal bloom prediction in the North Sea. Ecological Modelling, 221(2): 178–190

Sellner K G, Doucette G J, Kirkpatrick G J. 2003. Harmful algal blooms: causes, impacts and detection. Journal of Industrial Microbiology & Biotechnology, 30(7): 383–406

Smagorinsky J. 1963. General circulation experiments with the primitive equations: I. The basic experiment. Monthly Weather Review, 91(3): 99–165

Tang Qisheng, Su Jilan, Sun Song, et al. 2005. A study of marine ecosystem dynamics in the coastal ocean of China. Advance in Earth Sciences (in Chinese), 20(12): 1288–1299

Trancoso A R, Saraiva S, Fernandes L, et al. 2005. Modelling macroalgae using a 3D hydrodynamic-ecological model in a shallow, temperate estuary. Ecological Modelling, 187(2): 232–246

Villanoy L C, Azanza V R, Altemerano A, et al. 2006. Attempts to model the bloom dynamics of Pyrodinium, a tropical toxic dinoflagellate. Harmful Algae, 5: 156–183

Wan Zhenwen, Yuan Yeli. 1999. Developing a continuous medium dynamics model for ocean plankton ecosystem. Oceanologia et Lmnologia Sinica (in Chinese), 30(6): 663–670

Wan Zhenwen, Yuan Yeli. 2000. Study on turbulence closure of dynamics model for marine plankton ecosystem. Journal of Hydrodynamics (in Chinese), 15(2): 229–239

Wang Hongli, Feng Jianfeng, Shen Fei. 2002. Nonlinear dynamics research of the algal model in Bohai Sea. Ocean Technology (in Chinese), 21(3): 8–12

Wang Zonglin, Li Ruixiang, Zhu Mingyuan, et al. 2006. Study on population growth processes and interspecific competition of *Prorocentrum donghaiense* and *Skeletonema costatum* in semi-continuous dilution experiments. Advances in Marine Science (in Chinese), 24(4): 495–503

Wang Jinhua, Tang Hongjie, Wang Xiulin, et al. 2008. Effects of nitrate and phosphate on growth and nitrate reductase activity of *Prorocentrum donghaiense*. Chinese Journal of Applied & Environmental Biology (in Chinese), 14(5): 620–623

Wang Baodong, Zhan Run, Zang Jiaye. 2002. Distributions and transportation of nutrients in Changjiang River Estuary and its adjacent sea areas. Acta Oceanologica Sinica (in Chinese), 24(1): 53–58

Wang Qing, Zhu Liangsheng, Hu Jinpeng, 2010. A HAB mathematical model of competition between two algae species in the Yangtze River Estuary and its adjacent waters. Proceedings of the Special Workshop on Geoscience and Remote Sensing in the 2010 International Conference on Multimedia Technology, 3: 1276–1279

Xie Wenling. 2006. Community structure and dynamics of planktonic diatoms in typical areas of East China Sea [dissertation]. Xiamen: Xiamen University

Yanagi T, Yamamoto T, Koizumi Y, et al. 1995. A numerical simulation of red tide formation. Journal of Marine Systems, 6(3): 269–285

Yuan Dongliang, Zhu Jianrong, Li Chunyan, et al. 2008. Cross-shelf circulation in the Yellow and East China Seas indicated by MODIS satellite observations. Journal of Marine Systems, 70(1): 134–149

Zhang Chuansong, Wang Jiangtao, Zhu Dedi, et al. 2008. The preliminary analysis of nutrients in harmful algal blooms in the East China Sea in the spring and summer of 2005. Acta Oceanologica Sinica (in Chinese), 30(2): 153–159

Zhao Yanfang, Yu Zhiming, Song Xiuxian, et al. 2009. Effects of different phosphorus substrates on the growth and phosphatase activity of *Skeletonema costatum* and *Prorocentrum donghaiense*. Environmental Science (in Chinese), 30(3): 693–699

Zhou Mingjiang, Zhu Mingyuan. 2006. Progress of the Project "Ecology and Oceanography of Harmful Algal Blooms in China". Advances in Earth Science (in Chinese), 21(7): 673–679